Developmental Biology 397 (2015) 89–102

Contents lists available at ScienceDirect

Developmental Biology

journal homepage: www.elsevier.com/locate/developmentalbiology

# Abnormal development of placenta in HtrA1-deficient mice

Md. Zobaer Hasan [a], Muthi Ikawati [a,b], Jiraporn Tocharus [c], Masashi Kawaichi [a], Chio Oka [a,*]

[a] Laboratory of Gene Function in Animals, Nara Institute of Science and Technology, 8916-5 Takayama, Ikoma, Nara 630-0192, Japan
[b] Faculty of Pharmacy, Gadjah Mada University, Sekip Utara, Yogyakarta 55281, Indonesia
[c] Department of Anatomy, Faculty of Medicine, Chiang Mai University, Chiang Mai 50200, Thailand

ARTICLE INFO

*Article history:*
Received 27 March 2014
Received in revised form
14 October 2014
Accepted 18 October 2014
Available online 27 October 2014

*Keywords:*
HtrA1
Placenta
Preeclampsia
Trophoblast
Maternal artery remodeling

ABSTRACT

Abnormal levels of High temperature requirement A1 (HtrA1) protein have been repeatedly observed in sera and placentas of preeclampsia patients. To understand the functions of HtrA1 in placentation and in the etiology of preeclampsia, we established *HtrA1*$^{-/-}$ mice. *HtrA1*$^{-/-}$ mice show intrauterine growth retardation, and their placentas are small due to a reduced size of the junctional zone and aberrant vascularization in the labyrinth at the mid-gestation stage. HtrA1 is expressed by *Tpbpa*-positive trophoblast precursors in the outer ectoplacental cone and junctional zone from embryonic day 7.5 to 10.5. In the *HtrA1*$^{-/-}$ placenta, *Tpbpa*-positive cell precursors are decreased in the early stage. Spongiotrophoblasts and glycogen trophoblast cells, both of which differentiate from *Tpbpa*-positive precursors, are consequently decreased in the junctional zone. Fewer spiral artery-associated trophoblast giant cells, another cell type derived from *Tpbpa*-positive precursors, invade the decidua and associate with maternal arteries in the *HtrA1*$^{-/-}$ placenta than in the wild type placenta. Maternal arteries in the *HtrA1*$^{-/-}$ decidua have narrower lumens, thicker arterial walls, and more vascular smooth muscle cells remaining in the walls than those in the wild type decidua, indicating impaired remodeling of maternal arteries. These results indicate that HtrA1 plays important roles in the differentiation of trophoblasts from *Tpbpa*-positive precursors in the ectoplacental cone. Insufficient levels of HtrA1 cause poor placental development and intrauterine growth retardation, due to aberrant trophoblast differentiation and consequent defects in maternal artery remodeling, and may contribute to the onset of preeclampsia.



## Introduction

High Temperature Requirement A (HtrA) is a serine protease family that is highly conserved from bacteria to humans. The key feature of this family is the combination of a catalytic serine protease domain with one or more C-terminal PDZ domains (Clausen et al., 2002). Mammals have four HtrA proteins. HtrA2 is distinct from other three: it is localized in the mitochondria, involved in quality control of proteins, and related to the pathogenesis of Parkinson's disease (Strauss et al., 2005). HtrA1, 3 and 4 have similar domain structures which include a secretory signal sequence, an IGFBP domain and a Kazal-type protease inhibitor domain in the N-terminal region. Although the physiological function of HtrA1 remains unclear, human HtrA1 has been linked with the pathogenesis of osteoarthritis (Hu et al., 1998), rheumatoid arthritis (Grau et al., 2006), CARASIL (cerebral autosomal recessive arteriopathy with subcortical infarcts and leukoencephalopathy)(Hara et al., 2009), age-related macular degeneration (Dewan et al., 2006; Yang et al., 2006) and cancers (Baldi et al., 2002; Chien et al., 2004; Mullany et al., 2011). HtrA1 digests several extracellular matrix proteins such as decorin, biglycan, fibronectin, fibromodulin and collagens (Tsuchiya et al., 2005; Grau et al., 2006). HtrA1 inhibits TGF-$\beta$ signaling in a protease activity-dependent manner (Oka et al., 2004; Hara et al., 2009). Although several mechanisms underlying this inhibitory activity have been suggested (Launay et al., 2008; Shiga et al., 2011; Graham et al., 2013), the precise mechanism is not yet understood.

HtrA1 is expressed most abundantly in the placenta and its expression is developmentally regulated (Nie et al., 2003; Oka et al., 2004; Nie et al., 2005). Abnormal elevation of HtrA1 has been repeatedly observed in the serum (Inagaki et al., 2012; Marzioni et al., 2012; Zong et al., 2013) and placenta (Inagaki et al., 2012) of patients with preeclampsia (PE), a pregnancy-associated multisystem disorder that is clinically diagnosed by hypertension and proteinuria (Steegers et al., 2010). In contrast, it has also been reported that total HtrA1 level decreases in the PE placenta with intrauterine growth restriction (Lorenzi et al., 2009;

*Abbreviations:* HtrA1, High temperature requirement A1; TGF-$\beta$, Transforming growth factor–beta; FGF, Fibroblast growth factor

* Corresponding author. Tel.: +81 743 72 5532; fax: +81 743 72 5539.
*E-mail address:* coka@bs.naist.jp (C. Oka).

http://dx.doi.org/10.1016/j.ydbio.2014.10.015
0012-1606/

Zong et al., 2013). These observations suggest that HtrA1 contributes to the normal development of the placenta and to the pathogenesis of PE. PE affects 2–8% of human pregnancies and accounts for 9–26% of pregnancy-related mortality worldwide (Khan et al., 2006; Duley, 2009). Although the pathogenesis of PE has not been fully elucidated, inadequate development and/or function of the placenta in early pregnancy may be the key cause of PE (Redman and Sargent, 2005; Steegers et al., 2010). Specifically, defective trophoblast invasion and subsequent inadequate maternal spiral artery remodeling are considered to be the first steps in the development of PE. During normal placentation, fetal cytotrophoblasts invade into the maternal decidua and align with uterine spiral arteries. The invading trophoblasts remodel maternal arteries by replacing the maternal endothelium and promote loss of smooth muscle cells, which results in artery dilation and an increase in blood flow. Impairment of maternal artery remodeling leads to placental ischemia and hypoxia. Uneven blood flow to portions of the placenta causes an ischemic-reperfusion insult and produces oxidative stress (Redman and Sargent, 2005).

Although the architecture of the mouse placenta is different from that of the human placenta in several respects (Rossant and Cross, 2001; McCarthy et al., 2011), the mouse placenta is considered as a good model to understand human placental development and disease. The placenta exerts its various roles through differentiated trophoblast cell lineages. In mouse, primary parietal trophoblast giant cells (P-TGCs) are the first cells to differentiate from the mural trophoectoderm after implantation (Simmons and Cross, 2005; Hu and Cross, 2010). At a later stage, the ectoplacental cone (EPC), which is derived from the polar trophoectoderm, gives rise to all the remaining trophoblast cell types of the placenta. Among these, spongiotrophoblasts (SpTs) and their derivatives, glycogen trophoblast cells (GlyTCs), are the major cell components of the junctional zone. The EPC also generates four subtypes of trophoblast giant cells (TGCs). Spiral artery-associated trophoblast giant cells (SpA-TGCs), which are analogs of invasive extravillous trophoblasts (EVTs) in human, invade into the maternal decidua, and remodel maternal arteries (Adamson et al., 2002; Hu and Cross, 2010, 2011). The other three TGC subtypes show distinct functions, unique gene expression patterns and different locations within the placenta (Simmons and Cross, 2005; Simmons et al., 2007): secondary parietal TGCs (P-TGCs) line the boundary between the fetal and maternal placentas and are in direct contact with maternal blood; canal-associated TGCs (C-TGCs) regulate maternal vasculature and physiology; and sinusoidal TGCs (S-TGCs) are located within the sinusoidal spaces of the labyrinth and modulate growth factors and hormones.

To understand the function of HtrA1 in normal development of the placenta and its involvement in the etiology of PE, we generated *HtrA1* gene knockout mice. *HtrA1*$^{-/-}$ mice showed developmental defects including a small placenta and intrauterine growth retardation, which were attributed to reductions in the number of SpTs and GlyTCs in the junctional zone and in the number of SpA-TGCs invading into maternal spiral arteries. These abnormalities originate from defects in cell fate determination and differentiation of trophoblast precursors in the EPC.

## Materials and methods

### Mice

*HtrA1*$^{-/-}$ mice were produced (Tsuchiya et al., 2005) by the conventional homologous recombination method using RF8 embryonic stem cells derived from 129/TerSV mice (Meiner et al., 1996). The structure of the targeting vector, the method of PCR genotying and the preliminary characterization of *HtrA1*$^{-/-}$ mice were described previously (Supplementary data in Jones et al., 2011). The absence of HtrA1 mRNA and protein in the knockout mice was confirmed (Fig. S1; see also Supplementary data in Jones et al., 2011). Mice used in this study were initially bred on a mixed 129/Sv and C56BL/6 background. The strain was subsequently backcrossed into BALB/c background more than 10 generations. Unless otherwise indicated, the mice used in this study had a mixed 129/Sv and C56BL/6 background. Data presented in Fig. 1B and some in supplementary data are results of experiments done on mice backcrossed to the BALB/c background. Pairs of *HtrA1*$^{+/+}$ or *HtrA1*$^{-/-}$ mice were mated to obtain placentas, embryos and pups of *HtrA1*$^{+/+}$ or *HtrA1*$^{-/-}$ genotype, respectively. Noon on the day of the appearance of the vaginal plug was set as embryonic day 0.5 (E0.5). All animal experiments were approved by the animal welfare sub-committee of Nara Institute of Science and Technology.

### Histology

Pregnant mice were sacrificed by an overdose of pentobarbital and perfused with 4% paraformaldehyde (PFA) in phosphate-buffered saline (PBS) at E9.5, E10.5, E12.5, E14.5 and E16.5. Placentas were dissected and fixed with 4% PFA/PBS overnight at 4 °C and then washed with PBS. For paraffin blocks, washed tissues were dehydrated through a graded ethanol series and xylene, and embedded in paraffin wax. Paraffin sections (5-μm thick) were de-waxed in xylene, rehydrated in an ethanol series, and subjected to hematoxylin and eosin (HE) or periodic acid Schiff (PAS) staining according to standard protocols. To prepare frozen tissue blocks, the washed tissues were incubated in 30% sucrose/PBS overnight. They were then embedded in OCT compound (Sakura, Tokyo, Japan), frozen in liquid nitrogen, and stored at −80 °C until use. For in situ hybridization analysis, 12-μm-thick sections were prepared. In all experiments, the central parts of the placentas were analyzed. At least five wild type or *HtrA1*$^{-/-}$ placentas were examined for each embryonic day.

### In situ hybridization

The *HtrA1* probe (Oka et al., 2004) and *HtrA3* probe (Tocharus et al., 2004) were prepared as described. Probes for *Tpbpa* (Carney et al., 1993) and *Mash-2* (Guillemot and Joyner, 1993) were kind gifts from Dr. James Cross, as were those for *Pl1, Pl2* and *Plf* (Simmons et al., 2007) from Dr. David Simmons. Linearized plasmids were used as templates for preparing digoxigenin (DIG)-labeled RNA probes using a DIG-RNA labeling kit (Roche, Mannheim, Germany). In situ hybridization was performed as described (Tocharus et al., 2004) with some modifications. Briefly, de-waxed and rehydrated paraffin sections (12 μm thick) or frozen sections (12 μm thick) were fixed with 4% PFA/PBS, treated with 1 μg/ml proteinase K (Takara, Otsu, Japan) at 37 °C for 30 min, acetylated for 10 min in 0.25% (v/v) acetic anhydride (Wako Chemicals, Osaka, Japan), and hybridized with DIG-labeled probes overnight at 55 °C. Next, the sections were washed, blocked with a blocking solution (0.5% Block Ace (Dai Nippon Sumitomo Pharma, Osaka, Japan) and 20% goat serum (Sigma-Aldrich, St Louis, USA) in Tris-buffered saline (TBS)) for 1 h at room temperature, and then incubated with alkaline phosphatase-conjugated anti-DIG antibody (Roche) diluted (1/1000) in blocking solution overnight at 4 °C. The sections were washed and color was developed using NBT/BCIP.

### Immunohistochemistry

Paraffin sections were de-waxed and then boiled for 30 min to retrieve antigens either in citrate buffer (pH 6.0) for isolectin B4 or in Immuno-active (pH 9.0, Matsunami, Osaka, Japan) for smooth

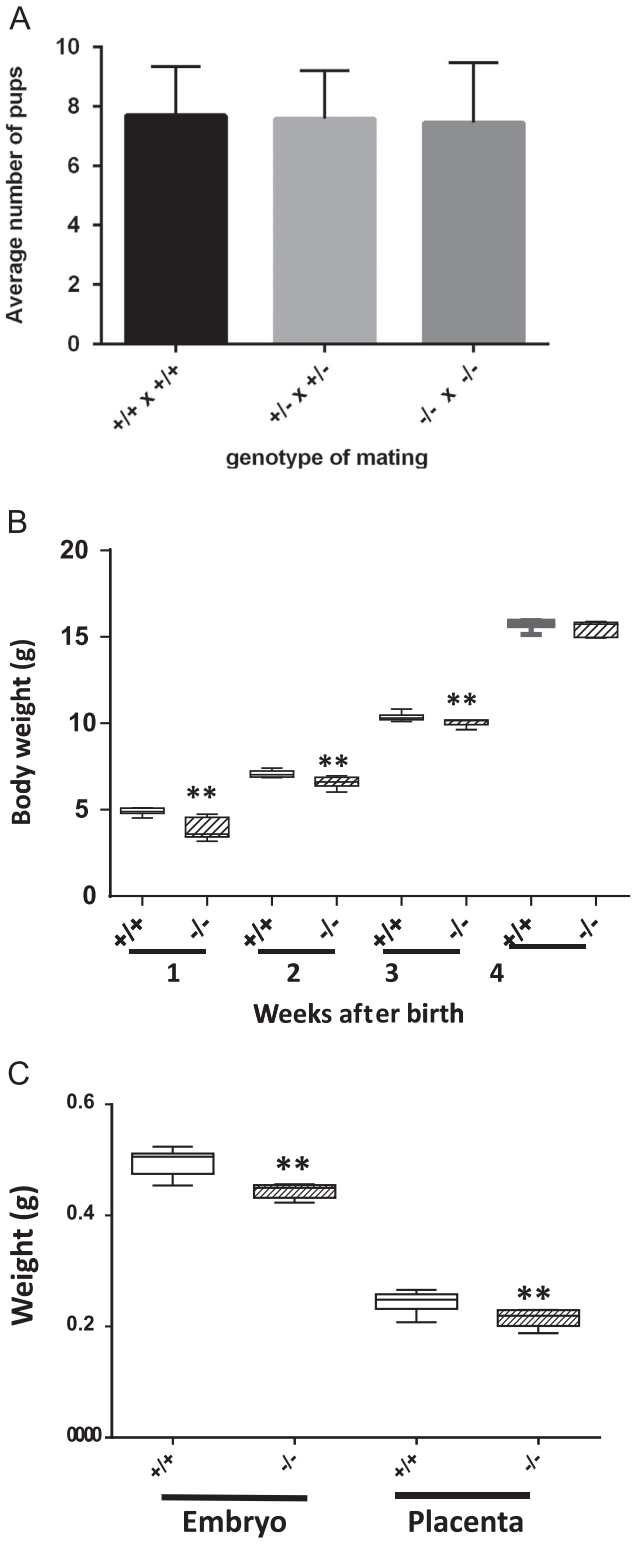


**Fig. 1.** Placentas, embryos and pups are small in *HtrA1*$^{-/-}$ mice. (A) Average number of pups born from crossing of *HtrA1*$^{+/+}$, *HtrA1*$^{+/-}$ and *HtrA1*$^{-/-}$ parents. Pairs of *HtrA1*$^{+/+}$, *HtrA1*$^{+/-}$ or *HtrA1*$^{-/-}$ mice were mated (each $n=11$) and the number of pups born was counted. (B) Body weight of wild type (*HtrA* $^{+/+}$) (n=10) and *HtrA1*$^{-/-}$ ($n=8$) pups after birth. Mice with the BALB/c background were used. (C) Weight of placentas and embryos from *HtrA1*$^{+/+}$ ($n=8$) and *HtrA1* $^{-/-}$ ($n=7$) mice at E14.5. P values were calculated by Welch's *t*-test. $^{**}P<0.01$. The boxes indicate the 25th and 75th percentile, the bands within these boxes indicate median values, and the ends of bars indicate the maximum and minimum values.

muscle α-actin. For isolectin B4 staining, the sections were blocked in 0.5% Block Ace in TBS for 30 min at room temperature and incubated with biotin-labeled isolectin B4 antibody (1/100, Vector Laboratories, Burlingame CA, USA) in PBS overnight at 4 °C. Subsequently, the sections were incubated with horseradish peroxidase-conjugated streptavidin (1/100, KPL, Gaithersburg MD, USA) in PBS containing 0.05% Tween 20 for 1 h at room temperature and then subjected to DAB development. For smooth muscle α-actin staining, the sections were blocked in 10% goat serum in PBS and incubated with rabbit polyclonal anti-smooth muscle α-actin antibody (1/500, Abcam, Cambridge, UK) in 1% bovine serum albumin/PBS overnight at 4 °C. They were then incubated with biotin-conjugated anti-rabbit IgG (1/200, Vector Laboratories) in 10% goat serum in PBS for 1 h at room temperature, incubated with the horseradish peroxidase-conjugated streptavidin for 1 h at room temperature, and finally subjected to DAB development.

### *Histomorphometric measurements and statistical analysis*

Three sections per placenta at 100-μm intervals from the central region near the site of umbilical cord attachment were analyzed. The area and diameter were measured using ImageJ software. Statistical significance was calculated by unpaired Student's *t*-test or Welch's *t*-test. The threshold of significance was set at $P<0.05$.

## Results

### *Deletion of HtrA1 results in intrauterine growth retardation*

*HtrA1*$^{-/-}$ mice were viable and fertile. *HtrA1*$^{+/+}$, *HtrA1*$^{+/-}$, and *HtrA1*$^{-/-}$ pups were born in the expected Mendelian ratio from mating of *HtrA1*$^{+/-}$ parents. Litter size was not affected by parental genotype (Fig. 1A and Fig. S2). However, *HtrA1*$^{-/-}$ mice were significantly smaller than wild type mice (Fig. 1B). Parents of homozygous *HtrA1*$^{-/-}$ mice were mated and the body weights of the progeny were examined every week after birth. Even in the *HtrA1*$^{-/-}$ newborn pups were significantly lighter than *HtrA1*$^{+/+}$ mice until the third week, the difference in body weight became non-significant in the fourth week (Fig. 1B). This difference in body weight in early life suggests that *HtrA1* deficiency affects placental or embryonic development. Indeed, when embryos and placentas were separately weighed at E14.5, both were significantly lighter in *HtrA1*$^{-/-}$ mice than in wild type mice (Fig. 1C).

### *Placental development is defective in HtrA1*$^{-/-}$ *mice*

We suspected that defects in the placenta were responsible for the smaller embryos and pups of *HtrA1*$^{-/-}$ mice. Next, therefore, we examined placenta sections histologically. *HtrA1*$^{-/-}$ placentas showed normal architecture, including three compartments (decidua basalis, junctional zone and labyrinth); however, they were smaller than wild type placentas at E12.5 (Fig. 2A and B). We measured the areas of the total placenta, junctional zone and labyrinth (Fig. 2S). At E12.5, the total area of *HtrA1*$^{-/-}$ placentas was significantly smaller than that of wild type placentas (Fig. 2S, top panel).

At E14.5, the phenotype became more prominent (Fig. 2C and D) and all three areas of the placenta were significantly reduced (Fig. 2S, middle panel). Paraffin sections of the placentas were stained with PAS (Fig. 2E and F). PAS stains GlyTCs, most of which usually reside in the junctional zone while some invade into the maternal decidua at E14.5. PAS staining showed the boundary between the junctional zone and labyrinth more clearly than HE staining, and hence the reduction of both areas in *HtrA1*$^{-/-}$ placentas (Fig. 2E and F). Next, we examined the cellular

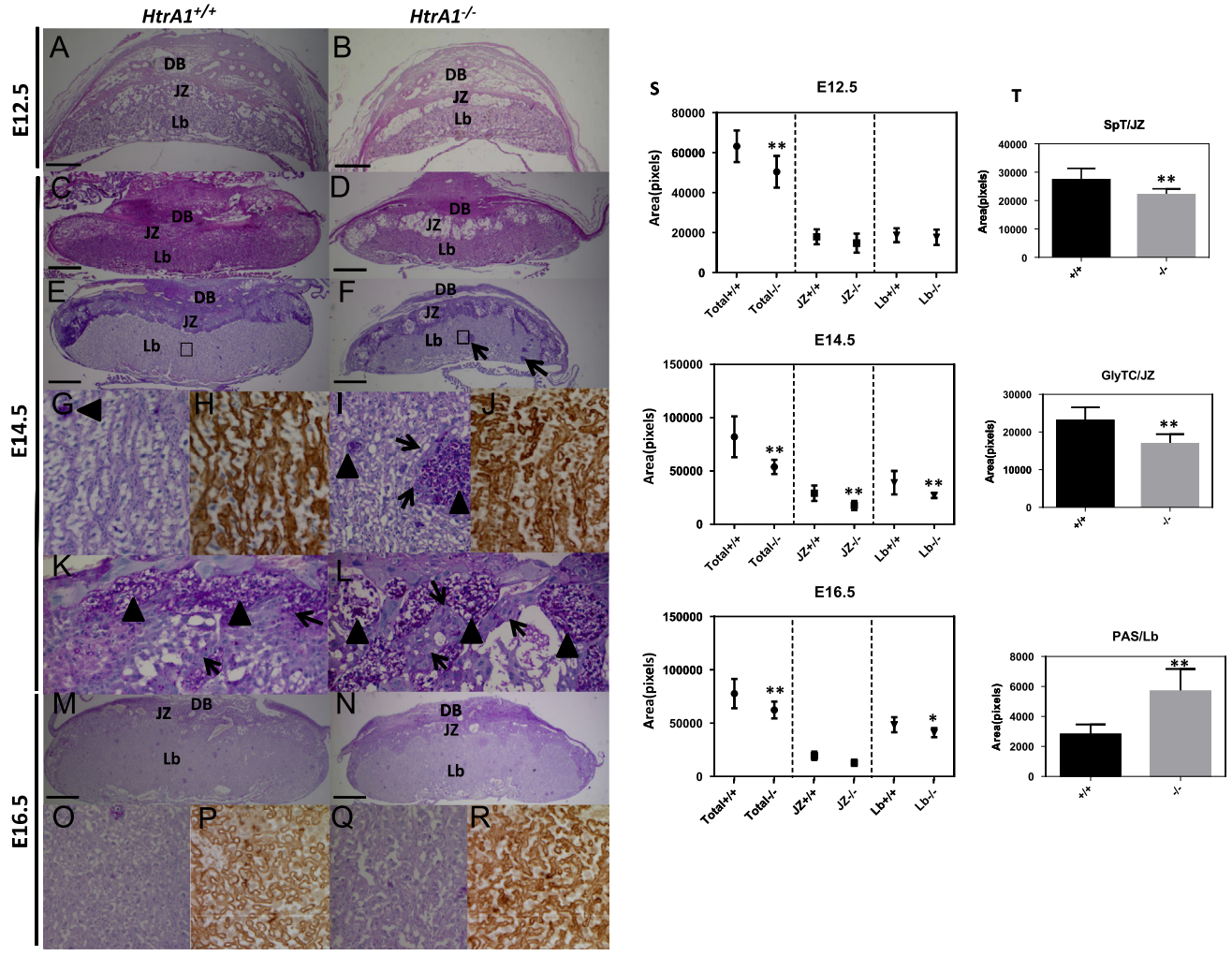


**Fig. 2.** HtrA1-deficient placentas have defects in development of junctional zone and labyrinth. (A-D) HE staining of sections from *HtrA1*$^{-/-}$ (B and D) and wild type (*HtrA1*$^{+/+}$) placentas (A and C) at E12.5 (A and B) and E14.5 (C and D). (E and F) PAS staining of sections from E14.5 *HtrA1*$^{-/-}$ (F) and *HtrA1*$^{+/+}$ (E) placentas. Arrows in F show large PAS-positive islands mislocalized in the labyrinth of an *HtrA1* $^{-/-}$ placenta. (G and I) Higher magnifications of boxed areas in E and F showing PAS-positive islands and structure of blood vessels in the labyrinth of *HtrA1* $^{-/-}$ (I) and *HtrA1*$^{+/+}$ (G) placentas. Arrowheads in G and I show PAS-positive islands, and arrows in I show PAS-negative SpT-like cells associated with an island. (H and J) Isolectin B4 staining of sections from E14.5 *HtrA1*$^{-/-}$ (J) and wild type (H) placentas, showing the structure of fetal vessels in the labyrinth. (K and L) Higher magnifications of the junctional zone of (E) and (F), showing PAS-negative SpTs (arrows) and PAS-positive GlyTCs (arrowheads) in *HtrA1*$^{-/-}$ (L) and *HtrA1*$^{+/+}$ (K) placentas. (M and N) PAS staining of sections from E16.5 *HtrA1*$^{-/-}$ (N) and *HtrA1*$^{+/+}$ (M) placentas. (O and Q) Higher magnifications of the labyrinth of (M) and (N). Abnormal vessel formation in *HtrA1*$^{-/-}$ labyrinth had mostly disappeared on E16.5. (P and R) Isolectin B4 staining of sections showing the labyrinth of E16.5 *HtrA1*$^{-/-}$ (R) and *HtrA1*$^{+/+}$ (P) placentas. Structure of vessels is almost normal in *HtrA1*$^{-/-}$ placentas. (S and T) Sections represented in A-F and K-N were analyzed morphometrically. (S) Areas of total placenta, junctional zone (JZ) and labyrinth (Lb) at E12.5, E14.5 and E16.5 of *HtrA1*$^{-/-}$ and *HtrA1*$^{+/+}$ placentas. (T) Area occupied by SpTs in the junctional zone (SpT/JZ), area occupied by GlyTCs in the junctional zone (GlyTC/JZ), and area of total PAS-positive trophpblast islands in the labyrinth (PAS/Lb) of E14.5 placentas. Five placentas from each genotype and three different sections from each placenta were analyzed. P values were calculated by Welch's *t*-test. $^{*}=P<0.05$, $^{**}=P<0.01$. Results are presented as mean+SD. DB, decidua basalis; JZ, junctional zone; Lb, labyrinth. Black scale bars=1000 μm. White scale bars=50 μm.

components of the junctional zone. The junctional zone is mainly composed of SpTs and GlyTCs at E14.5. SpTs are not stained with PAS and appear gray in the cytoplasm with large nuclei, while GlyTCs are stained magenta with small and dense nuclei and vacuoles in the cytoplasm (Fig. 2K and L). The area occupied by either SpTs (Fig. 2T, top) or GlyTCs (middle) in the junctional zone was decreased in *HtrA1*$^{-/-}$ placentas. There were clusters of PAS-positive cells in the labyrinth (Fig. 2E and F). These PAS-positive islands were larger and more numerous in *HtrA1*$^{-/-}$ placentas than in wild type placentas (Fig. 2E and F). Higher magnification showed that the islands contained PAS-positive GlyTCs and a small number of PAS-negative SpT-like cells (Fig. 2G and I). The total area of the PAS-positive islands in the labyrinth was quantitated (Fig. 2T, bottom), revealing that the placentas of *HtrA1*$^{-/-}$ mice had more PAS-positive cells in the labyrinth. In the normal placenta, a small number of GlyTGs are left behind in the labyrinth at E14.5. The increased and persistent mislocalization of PAS-positive trophoblasts in the labyrinth observed in *HtrA1*$^{-/-}$ placentas indicates defective differentiation of trophoblasts.

PAS stains the basement membrane of blood vessels, and the structures of blood vessels were clearly revealed by PAS staining. In *HtrA1*$^{-/-}$ placentas, the alignments of blood vessels in the labyrinth were more random than those in *HtrA1*$^{+/+}$ placentas (Fig. 2G and I). To gain more detailed insight, placentas were stained with isolectin B4, which specifically stains fetal blood vessels. The fetal vessels of *HtrA1*$^{+/+}$ placentas looked elongated with long straight segments, and ran parallel to each other toward the decidua (Fig. 2H), while those of *HtrA1* $^{-/-}$ placentas were more randomly aligned (Fig. 2J).

At E16.5, PAS staining showed that the *HtrA1*$^{-/-}$ placenta was still significantly smaller than wild type placenta (Fig. 2M and N), although the difference was less marked than at E14.5 (Fig. 2S, bottom panel). The area and number of PAS-positive islands in labyrinth of *HtrA1*$^{-/-}$ placentas were reduced and not different

from those of wild type placentas (Fig. 2M and N), while the random alignment of blood vessels in the *HtrA1*$^{-/-}$ labyrinth had mostly disappeared (Fig. 2O-R).

*Expression of HtrA1 and HtrA3 in placenta*

Both HtrA1 and HtrA3 are expressed most abundantly in the placenta among adult mouse tissues (Oka et al., 2004; Tocharus et al., 2004), and their expression patterns have been immunohistologically analyzed (Nie et al. 2005, 2006b). However, since these proteins are secreted, in situ hybridization is necessary to precisely identify cells expressing HtrA1 and HtrA3. To understand the function of HtrA1 in development of the placenta and the possible compensation for HtrA1 function by HtrA3 in *HtrA1*$^{-/-}$ placentas, we re-examined HtrA1 and HtrA3 expression patterns by in situ hybridization (Fig. 3). We also carried out in situ hybridization using various probes specific to trophoblast cell lineages in order to precisely identify cells that express HtrA1 (Fig. 3A-C).

At E7.5, HtrA1 was expressed strongly by cells in the decidua capsularis and weakly in the outer layer of the EPC (Fig. 3A), whereas HtrA3 was very faintly expressed in a small number of cells in the decidua basalis (data not shown). At E8.5, HtrA1 expression became more prominent in the outer EPC and continued in the decidua capsularis (Fig. 3D and H). HtrA1 expression

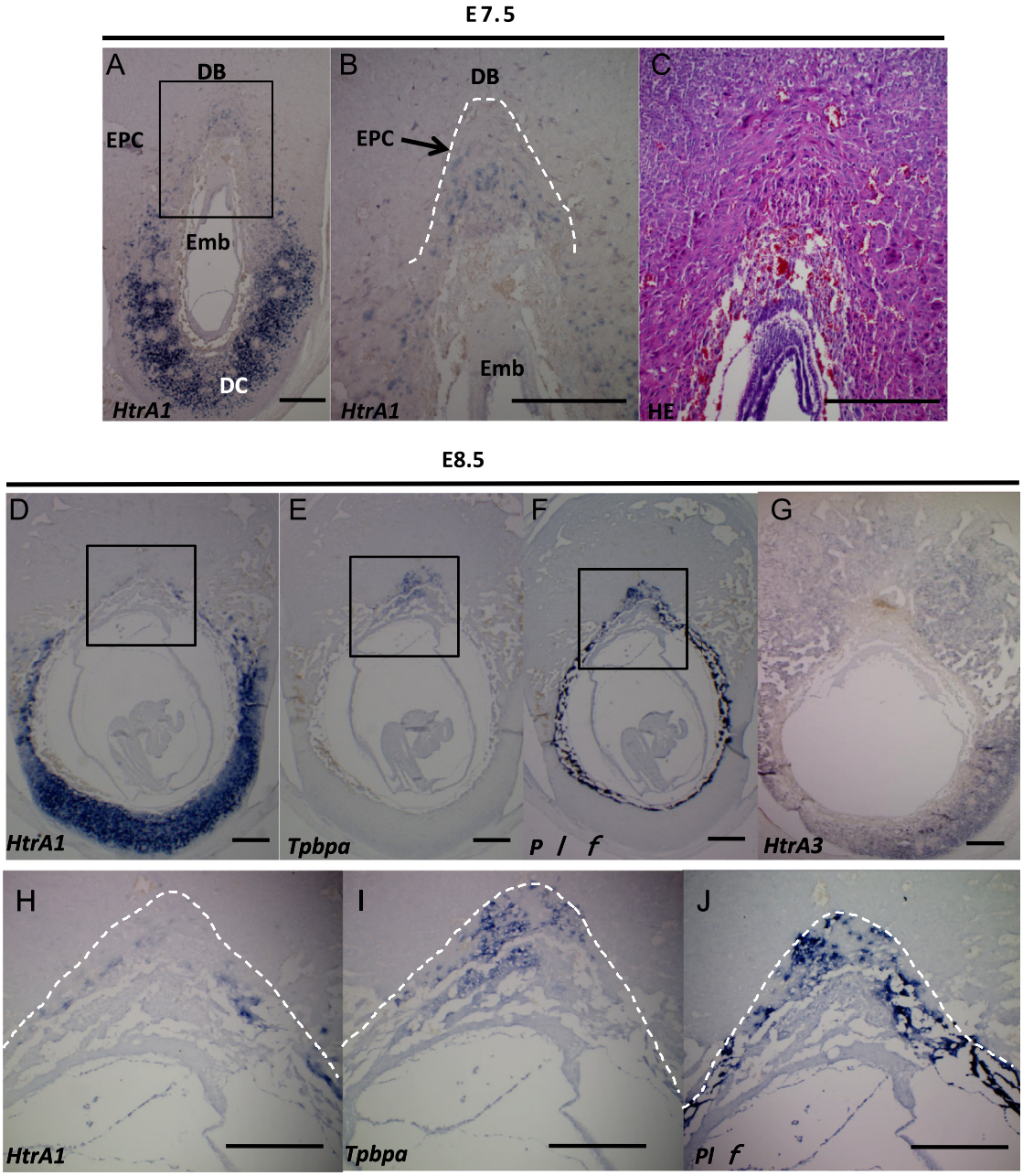


**Fig. 3.** Expression of HtrA1 and HtrA3 in developing mouse placenta at E7.5, E8.5 and E9.5. In situ hybridization was carried out on serial sections from E7.5 (A and B), E8.5 (D-J) and E9.5 (K-Y) placentas using probes for *HtrA1* (A, B, D, H, K, Q and T), *HtrA3* (G, P, S and Y), *Tpbpa* (E, I, L and U), *Plf* (F, J, M and V), *Pl1* (N, R and W) and *Pl2* (O and X). HE staining of a serial section adjacent to B is shown in C. Boxed areas in A and D-F are magnified in B and H-J, respectively. Higher magnifications of the junctional zone (black boxed area) in K-P are shown in T-Y, respectively. Higher magnifications of the decidua capsularis (white boxed area) in K, N and P are shown in Q, R and S, respectively. The mesometrial side is at the top and the fetal or anti-mesometrial side is at the bottom. EPC, ectoplacental cone; DB, decidua basalis; DC, decidua capsularis; Emb,embryo. Dotted lines in B, H, I and J indicate the boundary between the EPC and the maternal decidua. Dotted lines in T-Y indicate the boundary between the junctional zone and the decidua. Scale bars=500 μm.

in the outer EPC was confirmed by in situ hybridization with *Tpbpa* and *Plf* as probes. *Tpbpa* is a marker of the EPC and is expressed by progenitors of SpTs (Simmons and Cross. 2005), and *Plf* is a marker of secondary TGCs, which are in the outermost layer of the EPC at this stage (Simmons et al. 2008). HtrA1 expression was observed in the area where *Tpbpa*-positive or *Plf*-positive cells existed (Fig. 3E, F, I and J). At E9.5, HtrA1 expression was restricted to a thin outer layer of cells in the junctional zone which zone is

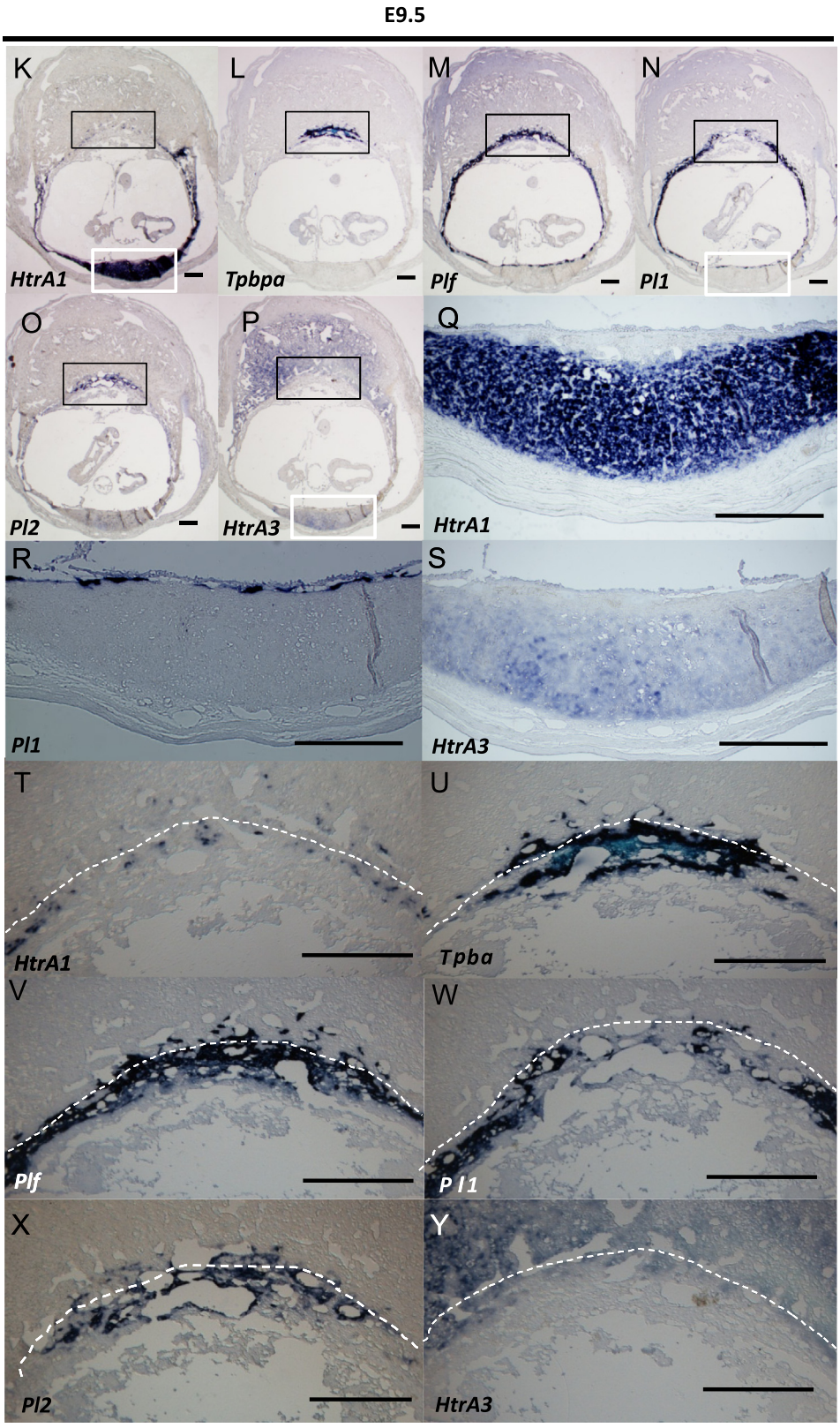


**Fig. 3.** (*continued*)

differentiated from the EPC (Fig. 3K, T). In situ hybridization of E9.5 placenta with the *Tpbpa* probe confirmed again that HtrA1 was expressed by trophoblast lineage cells in the junctional zone (Fig. 3K, L, T and U). The HtrA1-expressing cells (Fig. 3T) were also positive for other trophoblast cell lineage markers such as *Plf* and *Pl2* (Fig. 3V and X). *Plf*-positive trophoblast cells migrating into the decidua are defined as SpA-TGCs. Therefore, HtrA1-expressing cells in the decidua near the junctional zone (Fig. 3T) are probably SpA-TGCs. Primary trophoblast giant cells are the first trophoblast cell lineage; they differentiate at around E6.5 from the mural trophectoderm, demarcate the border between fetal and maternal tissues, and express *Pll* (Fig. 3N, R and W). The HtrA1-expressing cells in the decidua capsularis (Fig. 3K and Q) were negative for *Pl1* (Fig. 3R), indicating that primary TGCs do not express HtrA1. On the other hand, HtrA3-expressing cells (Fig. 3P, S and Y) were negative for all these trophoblast markers. HtrA3 expression, therefore, is restricted to decidual cells.

From E10.5 to E12.5, HtrA1-expressing cells were also detected inside the decidua basalis, closed to the junctional zone, and some HtrA1-expressing cells in the decidua basalis were associated with maternal arteries (Fig. S4B, C, G, and H, arrows). HtrA1 expression in the decidua capsularis decreased at E10.5 but was still very strong compared to that in the junctional zone (Fig. S4A). HtrA3 expression gradually increased and was detected diffusely in the decidual cells in both the basal and capsular regions in this period (Fig. S4D, E and I). Some HtrA3-expressing cells densely surrounded maternal arteries in the decidua on E10.5 and E12.5 (Fig. S4F and J, arrows).

*Tpbpa-positive cells decrease in the junctional zone but increase in the labyrinth of HtrA1$^{-/-}$ placenta*

*HtrA1$^{-/-}$* placentas showed a remarkable decrease in SpTs and GlyTCs in the junctional zone at E14.5 (Fig. 2). SpTs and GlyTCs originate from the same *Tpbpa*-positive precursors that are present in the outer layer of the EPC at E8.5. The cells expressing *Tpbpa* differentiate into SpTs at around E10.5 and GlyTCs differentiate from SpTs at around E12.5 (Simmons et al., 2007). *Tpbpa* expression continues in SpTs and GlyTCs at E14.5. Since HtrA1-expressing cells were positive for *Tpbpa* at E8.5 and E9.5 (Fig. 3H, I, T and U), we next examined whether the absence of HtrA1 affects *Tpbpa*-positive cell lineages. At E10.5, there were fewer *Tpbpa*-expressing cells in *HtrA1$^{-/-}$* placentas (Fig. 4B and D) than in *HtrA1$^{+/+}$* placentas (Fig. 4A and C). This decrease was also observed at later stages. *HtrA1$^{-/-}$* placentas at both E12.5 and E14.5 showed a decrease in *Tpbpa*-positive cells in the junctional zone (Fig. 4E-L). These results strongly suggest that defects in *Tpbpa*-positive precursor cells result in the reduction of SpTs and GlyTCs observed in the junctional zone. PAS-positive trophoblast islands in the labyrinth, which increased significantly in *HtrA1$^{-/-}$* placenta at E14.5, were also positive for *Tpbpa* (Fig. 4G, H, K and L, arrows). SpTs and TGCs differentiate from a common precursor in the EPC. The cell fate decision to differentiate into SpTs is positively regulated by the transcription factor Mash-2, and *Tpbpa*-positive SpTs were absent in *Mash-2* KO mice (Guillemot et al., 1994). *Mash-2* expression was detected in both junctional zone and labyrinth at E10.5 (Fig. 4M-P), as previously reported (Nakayama

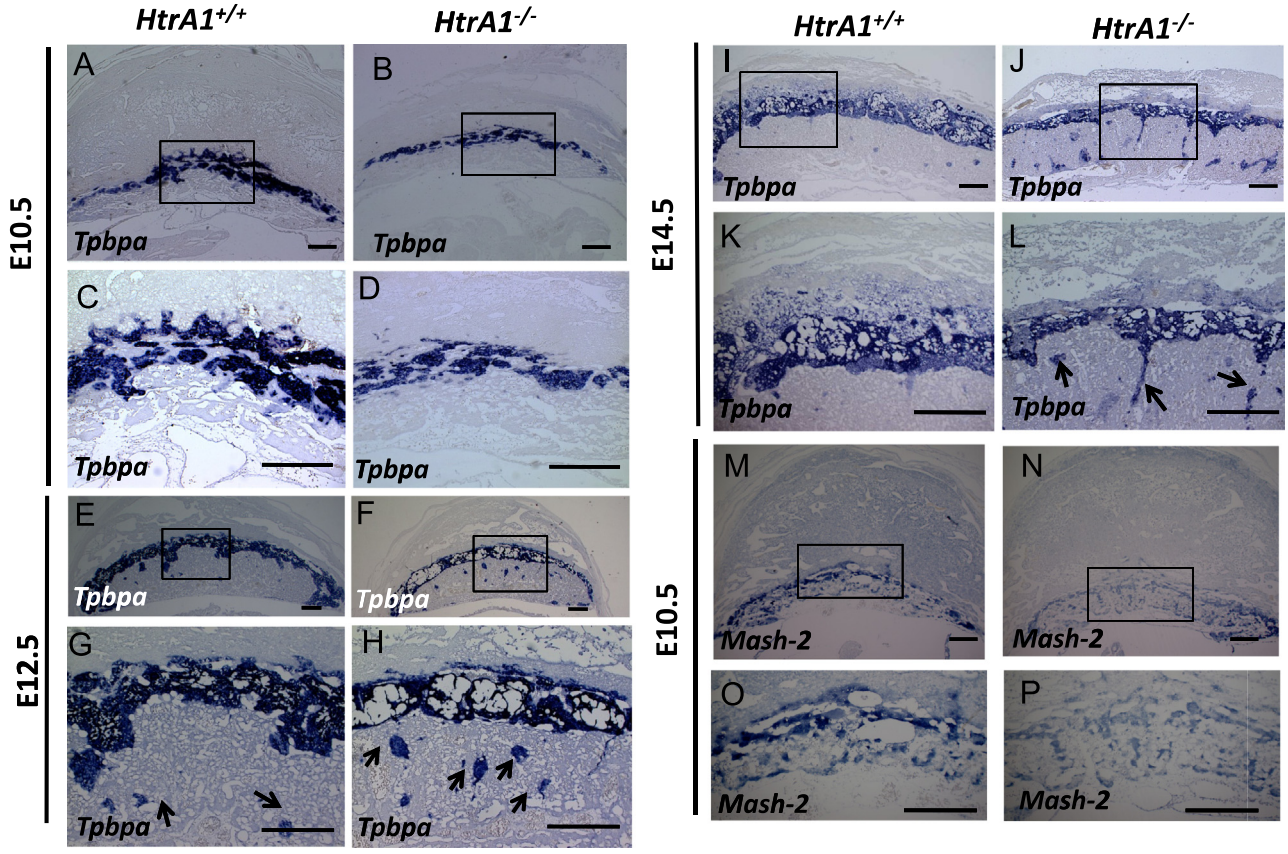


**Fig. 4.** Absence of HtrA1 reduces *Tpbpa*-positive cells in the junctional zone. In situ hybridization of sections from *HtrA1$^{+/+}$* (first and third columns) and *HtrA1$^{-/-}$* (second and fourth columns) placentas at E10.5 (A-D and M-P), E12.5 (E-H) and E14.5 (I-L) was performed using the *Tpbpa* probe (A-L) and *Mash*-2 probe (M-P). Boxed areas in A, B, E, F, I, J, M and N are magnified in C, D, G, H, K, L, O and P, respectively. *HtrA1$^{-/-}$* placentas had fewer *Tpbpa*-positive and *Mash-2*-positive cells in the junctional zone compared to *HtrA1$^{+/+}$* placentas. PAS-positive islands in the labyrinth were also *Tpbpa*-positive (arrows in G, H and L) and increased in *HtrA1$^{-/-}$* placentas (F, H, J and L) as compared to wild type placentas (E, G, I and K). Scale bars=500 μm.

et al., 1997). *Mash-2*-positive cells in *HtrA1*$^{-/-}$ placentas (Fig. 4N and P) were reduced compared to *HtrA1*$^{+/+}$ placentas (Fig. 4M and N). The reduction was more prominent in junctional zone than in labyrinth (Fig. 4O and P), supporting the idea that SpT differentiation from EPC precursors was defective in *HtrA1*$^{-/-}$ placentas. All these data indicate that *HtrA1*$^{-/-}$ placentas have abnormalities in the differentiation of SpTs and GlyTCs from *Tpbpa*-positive precursor cells. To reveal whether other trophoblast subtypes were affected by deletion of the *HtrA1* gene, we examined E9.5 placentas from *HtrA1*$^{-/-}$ mice by in situ hybridization with *Plf*, *Pl2* and *Pl1* probes, which are commonly used for trophoblast subtype identification.

### *SpA-TGCs decrease and maternal artery remodeling is compromised in the absence of HtrA1*

*Plf*-positive cells are differentiated from *Tpbpa*-positive cells and *Plf* is a marker for secondary P-TGCs, SpA-TGCs, and C-TGCs at later stages around E12.5 and E14.5. SpA-TGCs invade into the decidual tissues and associate with maternal arteries (Simmons et al., 2007). In E9.5 *HtrA1*$^{-/-}$ placentas, fewer *Plf*-positive cells invaded into the decidua (Fig. 5C and D) than did so in *HtrA1*$^{+/+}$ placentas (Fig. 5A and B). Similar defects in invasion and arterial association of *Plf*-positive SpA-TGCs were observed in the E12.5 *HtrA1*$^{-/-}$ decidua (Fig. 5I-L). The decrease in SpA-TGCs is clearly depicted in Fig. 7M, which shows the number of *Plf*-positive cells surrounding maternal arteries in *HtrA1*$^{-/-}$ and wild type placentas at E9.5. The association of SpA-TGCs with maternal arteries induces remodeling of the arteries, which results in enlargement of the arterial cavity to increase blood flow to the fetal placenta (Adamson et al., 2002). We measured the lumen diameters of arteries which were associated with *Plf*-positive cells at E9.5 (Fig. 5N). The data showed that although some SpA-TGCs attached to maternal arteries in the *HtrA1*$^{-/-}$ placentas, the association was not enough to induce enlargement of the cavity.

At an early stage, around E9.5, invading SpA-TGCs and some vessel-associated SpA-TGCs express *Tpbpa* (Fig. 3U and V; (Mold et al., 2012)). To confirm the results with *Plf*, we did performed in situ hybridization with the *Tpbpa* probe. Fewer *Tpbpa*-positive cells invaded into the decidua and associated with maternal arteries in the *HtrA1*$^{-/-}$ placentas at E9.5 than in the *HtrA1*$^{+/+}$ placentas (Fig. 5E-H).

During remodeling, the vessel walls of maternal spiral arteries become thin and lumen diameters widen. At E12.5, HE staining of maternal arteries in the distal part of the decidua showed that the lumen of arteries was narrower, and the walls of arteries were thicker, in *HtrA1*$^{-/-}$ placentas than in *HtrA1*$^{+/+}$ placentas (Fig. 6A and B). Another aspect of spiral artery remodeling is the replacement of vascular smooth muscle cells in arterial walls by the invading trophoblasts. Arteries in the decidua of *HtrA1*$^{-/-}$ placentas had more vascular smooth muscle cells, which were labeled with anti-smooth muscle α-actin antibody, than those in *HtrA1*$^{+/+}$ placentas at E 9.5 (Fig. 6C and D). All these observations indicate that maternal spiral artery remodeling is defective in *HtrA1*$^{-/-}$ placentas. Consistent with those observations, the ratio of inner lumen diameter to outer diameter (LD/OD) was reduced in *HtrA1*$^{-/-}$ arteries at E12.5 and E14.5 (Fig. 6E).

### *Canal trophoblast giant cells increase in the absence of HtrA1*

*Pl2* is a lineage marker for C-TGCs and P-TGCs in the junctional zone and for S-TGCs in the labyrinth (Simmons et al., 2007). *Pl2*-positive cells increased markedly in the junctional zone of *HtrA1*$^{-/-}$ placentas at E9.5 (Fig. 7A-D) as well as E12.5 (Fig. 7 E-H). The number of *Pl2*-positive S-TGCs in the labyrinth did not differ between *HtrA1*$^{-/-}$ and wild type mice (Fig. 7G and H).

### *Differentiation of Tpbpa-positive cell lineages is preferentially affected in HtrA1*$^{-/-}$ *placenta*

So far we have described abnormal trophoblast populations in *HtrA1*$^{-/-}$ mice; decreased numbers of SpTs and GlyTCs in the junctional zone and of SpA-TGCs in the decidua, mislocalization of PAS-positive cells in the labyrinth, and an increase in *Pl2*-positive trophoblasts in the junctional zone. A common feature of these trophoblast cell lineages is that they differentiate from *Tpbpa*-positive precursors in the outer EPC (Simmons et al., 2007). To examine whether only the trophoblasts derived from *Tpbpa*-positive precursors were affected in *HtrA1*$^{-/-}$ placentas, we conducted in situ hybridization with *Pl1* as the probe. *Pl1* is a marker for primary P-TGCs, which originate from both *Tpbpa*-positive and -negative precursors. In situ hybridization of E9.5 (Fig. 7I-L) and E10.5 placentas (data not shown) showed that the number and distribution of *Pl1*-positive cells in *HtrA1*$^{-/-}$ placentas were similar to those in wild type placentas. This result suggests that *Tpbpa*$^{-}$positive cell lineages are preferentially affected by the loss of HtrA1.

### *Matrix metalloproteinase (MMP)-9 activity is reduced in HtrA1*$^{-/-}$ *placenta*

HtrA1 digests fibronectin and the digested fragments enhance the production of MMP-1 and MMP-3 in human synovial fibroblasts (Grau et al., 2006). Similarly, fibronectin fragments generated by α-chymotrypsin enhance the secretion of MMP-3 and MMP-9 in murine RPE cells (Grau et al., 2006; Austin, et al., 2009). However, MMP-2 production was not affected in either cell type by fibronectin fragments (Grau et al., 2006; Austin et al., 2009). We compared MMP activities by gelatin zymography of extracts from *Htr1*$^{+/+}$ and *HtrA1*$^{-/-}$ placenta at E10.5 (Fig. S5), when the MMP activities in placenta are highest during pregnancy (Fontana et al., 2012). Consistent with previous report (Fontana et al., 2012), MMP-9 and MMP-2 are the major MMPs in the placenta at this stage. Gelatin zymography indicated that MMP-9 activity was reduced in *HtrA1*$^{-/-}$ placentas, but MMP-2 activity was not affected (Fig. S5B), suggesting that the loss of HtrA1 activity suppressed the expression or activation of MMP-9. This decrease in MMP9 activity may compromise the migration of TGCs and the remodeling of maternal arteries.

### *Embryonic HtrA1 loss contributes to the abnormal phenotype of placentas*

To determine which HtrA1 deficiency, maternal or embryonic, contributed to the phenotype of the *HtrA1*$^{-/-}$ placenta, placentas derived from matings between different genotypic combinations were analyzed (Fig. S6). Placentas of *HtrA1*$^{-/-}$ females crossed with *HtrA1*$^{+/+}$ males were normal in size (Fig. S6 A-C, J-L and S-T) and showed normal maternal artery remodeling (Fig. S6M-O). In these placentas, the development of *Tpbpa*-positive SpTs and *Plf*-positive SpA-TGCs was also normal (Fig. S6 D-I and P-R). These data suggest that the loss of embryonic HtrA1 was the major cause of the abnormal development of the *HtrA1*$^{-/-}$ placenta.

## Discussion

Our in situ hybridization analysis revealed that *HtrA1* is expressed from E7.5 to E12.5 in two distinct regions: the decidua capsularis and the outer layer of EPC or the junctional zone (Fig. 4). The mRNA expression pattern at E7.5 is consistent with the protein distribution, reported previously (Nie et al., 2005), indicating that HtrA1 protein travels only a short distance after it is secreted.

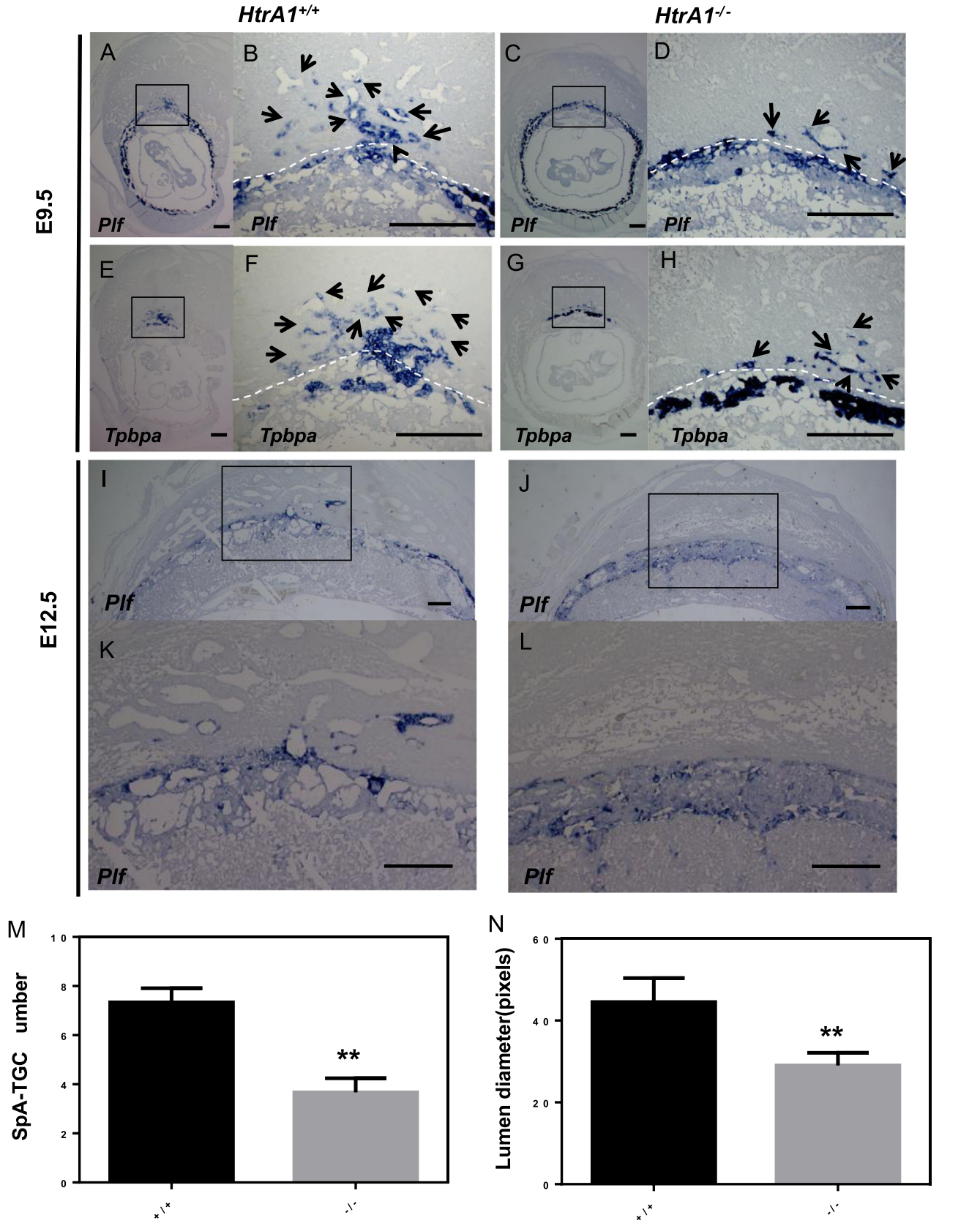


**Fig. 5.** Defective invasion of SpA-TGCs into the decidua in HtrA1-deficient placenta. (A-L) In situ hybridization of sections from *HtrA1*$^{+/+}$ (left) and *HtrA1*$^{-/-}$ (right) placentas at E9.5 (A-H) and E12.5 (I-L) were carried out using the *Plf* probe (A-D and I-L) and the *Tpbpa* probe (E-H). These probes detect SpA-TGCs in the decidua. Fewer *Plf*-positive (arrows in B and D) and *Tpbpa*-positive (arrows in F and H) cells invade into *HtrA1*$^{-/-}$ decidua than into *HtrA1*$^{+/+}$ decidua at E9.5. Fewer *Plf*-positive cells line maternal arteries in *HtrA1*$^{-/-}$ decidua (J and L) than in wild type decidua (I and K) at E12.5. Dotted lines indicate the boundary between the junctional zone and the maternal decidua. (M) Number of SpA-TGCs that had invaded into the decidua was counted in *HtrA1*$^{-/-}$ and wild type placentas. One section which had most *Plf*-positive cells and five placentas for each genotype were measured. (N) Lumen diameter of the SpA-TGC-associated arteries was measured in the decidua of *HtrA1*$^{-/-}$ and *HtrA1*$^{+/+}$ placentas at E9.5. More than five arteries for one placenta and three placentas for each genotype were measured. P values were calculated by Welch's T test. $^{**}=P<0.01$. Results are presented as mean+SD. Scale bars=500 μm.

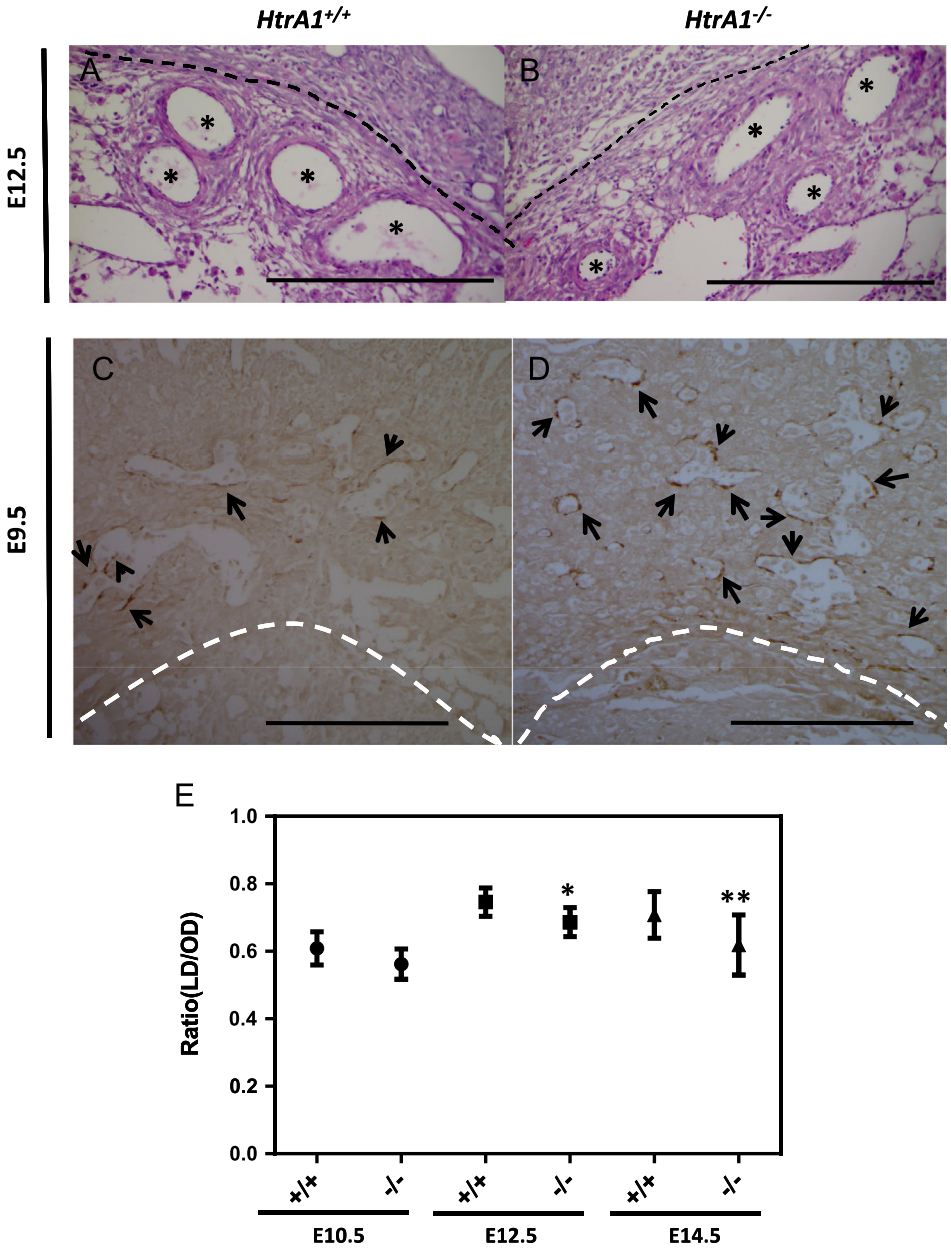


**Fig. 6.** Impaired maternal artery remodeling in *HtrA1*$^{-/-}$ placentas. (A and B) HE staining of a distal part of the decidua of E12.5 *HtrA1*$^{-/-}$ (B) and *HtrA1*$^{+/+}$ (A) placentas. Dotted lines in A and B indicate the boundary between the decidua and the myometrium. *HtrA1*$^{+/+}$ arteries have dilated lumens and thin walls (asterisks in A). In contrast, *HtrA1*$^{-/-}$ arteries have narrow lumens and thick walls (asterisks in B). (C and D) Immunostaining with anti-smooth muscle α-actin antibody of sections from E9.5 *HtrA1*$^{-/-}$ (D) and *HtrA1*$^{+/+}$ (C) placentas. More vascular smooth muscle cells associate with arteries in the decidua of *HtrA1*$^{-/-}$ placenta (arrows in D) as compared to *HtrA1*$^{+/+}$ placenta (arrows in C). Dotted lines in C and D show the boundary between the junctional zone and the maternal decidua. (**E**) Ratio of inner lumen diameter (LD) to outer diameter (OD) of maternal arteries in the distal part of the decidua of E10.5, E12.5 and E14.5 *HtrA1*$^{-/-}$ and *HtrA1*$^{+/+}$ placentas. More than five arteries from one placenta and five placentas for each genotype were measured at each time point. *P* values were calculated by Welch's *t*-test. $^{*}P<0.05$, $^{**}P<0.01$. Results are presented as mean±SD. Scale bars=500 μm.

HtrA1 protein is probably deposited in the ECM of the placenta, as it is in bone and cartilage (Tsuchiya et al., 2005). *HtrA1* mRNA in the whole placenta is first detected at E7.5, reaches its peak at E10.5, and quickly declines by E12.5 (Nie et al., 2005). This expression kinetics agrees well with the expression levels in the decidua capsularis, which is the major source of *HtrA1* mRNA (Fig. 3). A small number of cells in the EPC express *HtrA1* at E7.5. At E8.5, *HtrA1* mRNA expression in the EPC is increased in the cells localized in the outer layer. Those *HtrA1*-expressing cells also express *Tpbpa* and are therefore the precursors of SpTs and GlyTCs. At E9.5, the *HtrA1*-expressing cells are restricted to the outermost layer of the junctional zone, where *Tpbpa* is also expressed. At later stages, around E10.5 and E12.5, some *HtrA1*-expressing cells invade into the decidua and surround maternal vessels. These cells fit the definition of SpA-TGCs; indeed, they overlap with cells expressing *Plf*, a marker of SpA-TGCs at this stage. *HtrA3* expression starts one day after *HtrA1* expression. At E8.5, *HtrA3* expression is weakly detected in the decidua basalis and the decidua capsularis, and reaches its peak at E10.5 (Fig. 3). In the decidua basalis, *HtrA3* expression was still high at E12.5 when the expression of *HtrA1* had already decreased. This result is also consistent with a previous report (Nie et al., 2006b) showing that moderate *HtrA3* expression in the decidua basalis continues until the later stages of pregnancy. More importantly, *HtrA3* expression is restricted to maternal decidual cells and is not detected in any type of fetal trophoblast cell. In contrast, *HtrA1* is expressed in

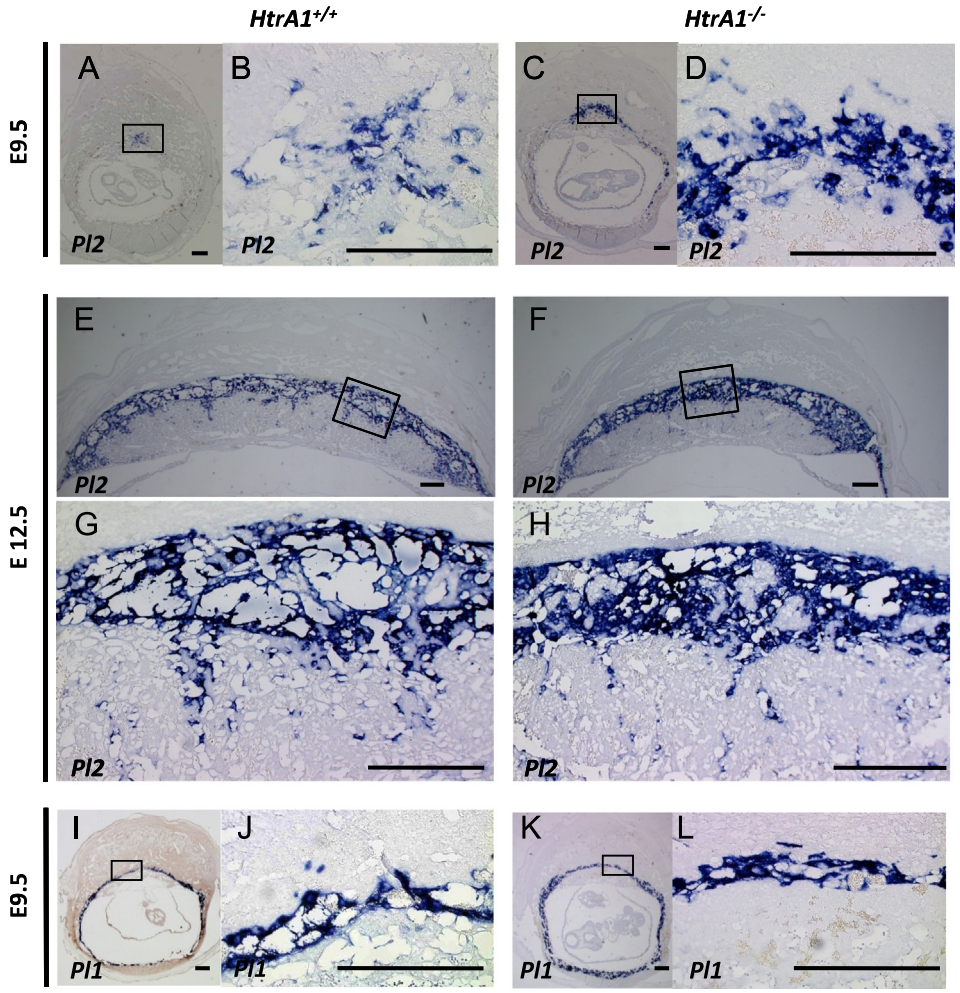


**Fig. 7.** C-TGCs are increased in *HtrA1*$^{-/-}$ placentas on E 9.5. In situ hybridization of sections from E9.5 (A-D and I-L) and E12.5 (E-H) *HtrA1*$^{-/-}$ (right) and *HtrA1*$^{+/+}$ (left) placentas was carried out using the *Pl2* probe, a C-TGC marker (A-H) and the *Pl1* probe, a P-TGCs marker (I-L). Higher magnifications of boxed areas in A, C, E, F, I and K are shown in B, D, G, H, J and L, respectively. JZ, junctional zone; Lb, labyrinth. Scale bars=500 μm.

both maternal cells in the decidua capsularis and fetal trophoblasts in the EPC. Collectively, these data show that HtrA1 and HtrA3 are expressed in a complementary manner, in different cells and in different periods during development of the mouse placenta. The *HtrA1*$^{-/-}$ placenta shows the most severe phenotypes at E14.5, but most abnormalities disappear by E16.5 (Fig. 2). It is possible that the function of HtrA1 is compensated for by HtrA3 at the later stages of pregnancy, when HtrA3 is dominant. Although HtrA1 expression in the decidua capsularis is very high, no significant abnormality was observed in this region throughout gestation (Fig. S3). Since both HtrA1 and HtrA3 are expressed in the cells of the decidua capsularis, HtrA3 may compensate the deficiency of HtrA1.

In human placenta, strong HtrA1 expression is detected in decidual cells in the first trimester (Nie et al., 2006a). At this stage, lower but moderate HtrA1 expression is also observed in trophoblasts (Nie et al., 2006a) such as villous cytotrophoblasts (CTBs), syncytotrophoblasts (STBs) and invasive EVTs. Villous CTBs provide precursors of all trophoblasts, as do cells in the EPC in mouse placenta. The existence of analogous progenitor cells in human and mouse (Fig. 2) expressing HtrA1 indicates an important function for HtrA1 in the differentiation of trophoblasts. STBs arise by fusion of differentiated CTBs, and EVTs differentiate from proliferating CTBs in CTB cell columns, where HtrA1 is expressed intensively in the first trimester (Marzioni et al., 2009). EVTs invade into the decidua (interstitial EVTs) and associate with maternal vessels (endovascular EVTs). HtrA1 expression in these ETVs is thought to be involved in cell invasion and maternal artery remodeling (Marzioni et al., 2009; Chen et al., 2014), functions similar to those that are expected for mouse *Tpbpa*-positive trophoblasts invading into the decidua and *Plf*-positive SpA-TGCs, two types of mouse trophoblasts expressing HtrA1 (Fig. 2).

The placenta of HtrA1-deficient mouse is small due to a reduction in size of the junctional zone and the labyrinth as well as an insufficiency of vasculogenesis in the labyrinth. These abnormalities probably cause intrauterine growth retardation. The principal defect in the *HtrA1*$^{-/-}$ placenta may be the decrease in *Tpbpa*-positive trophoblast precursors in the EPC at an early stage of placentation. This defect reduces SpT and GlyTC numbers, resulting in the small junctional zone, which is most prominent at E14.5. Ablation of *Tpbpa*-positive precursors by diphtheria toxin transgene expression results in the reduction of SpTs around E10.5 and of GlyTCs at later stages (Hu and Cross., 2011), in agreement with our finding that the reduction of SpTs and GlyTCs is caused by the loss of *Tpbpa*-positive precursor cells in the *HtrA1*$^{-/-}$ placenta. Although HtrA1 expression is not evident in the labyrinth throughout gestation, the development of the labyrinth is poor in the absence of HtrA1, suggesting that secondary mechanisms induce defects in the labyrinth. Poor development of the labyrinth has been reported as a secondary consequence of defects in SpTs in the junctional zone (Guillemot et al., 1995; Tanaka et al., 1997; Rodriguez et al., 2004; Arima et al., 2006). In the *HtrA1*$^{-/-}$

placenta, excessive *Tpbpa*-positive cells which are either PAS-positive or -negative remain in the labyrinth at E12.5 and E14.5, but disappear by E16.5 (Fig. 2). This mislocalization may be caused by a delay in cell migration to the junctional zone, and thus contribute to the reduction of GlyTCs and SpTs there. Similar mislocalization of trophoblasts has been observed previously in BPH/5 preeclampsia model mice (Dokras et al., 2006), heme oxigenase-1-deficient mice (Zhao et al., 2009), Cited1-deficient mice (Rodriguez et al., 2004), and in a mouse model of pregnancy diabetes (Salbaum et al., 2011); trophoblast mislocalization in these mice has been explained by aberrant differentiation of SpTs. These mice mostly show poor development of the labyrinth and intrauterine growth retardation. Excessive and persistent localization of trophoblast islands in the labyrinth may inhibit normal vessel formation and development of the labyrinth by physical hindrance. The mislocalized trophoblasts may also secrete factors such as pro- or anti-angiogenic factors that disturb the development of the labyrinth.

SpA-TGCs express HtrA1 and their numbers are reduced in the *HtrA1*$^{-/-}$ placenta. A lineage-tracing experiment using *Tpbpa-Cre* transgenic mice has revealed that all SpA-TGCs are derived from *Tpbpa*-positive precursors (Simmons et al., 2007). Diphtheria toxin-mediated ablation of *Tpbpa*-positive cells also led to a decrease in *Plf*-positive SpA-TGC number and insufficient maternal artery remodeling (Hu and Cross, 2011). *Plf*-positive SpA-TGCs migrate into the decidua, where they replace smooth muscle and endothelial cells of the maternal spiral artery. This remodeling of the artery enlarges the lumen diameter and increases blood flow to the fetal placenta, and is one of the most important mechanisms to prevent PE. We showed that the diameter of the spiral artery is narrower, and the arterial wall is thicker and contains more smooth muscle cells, in *HtrA1*$^{-/-}$ placenta than in *HtrA1*$^{+/+}$ placenta. These phenotypes represent compromised arterial remodeling and are probably caused by the reduction in migrating SpA-TGCs. In the remodeling process, protease activity is required to digest ECM proteins surrounding arteries (Harris and Aplin, 2007; Palei et al., 2013). Since HtrA1 effectively degrades ECM proteins such as fibronectin, decorin, biglycan, and collagens in vitro (Tsuchiya et al., 2005; Grau et al., 2006), HtrA1 secreted from SpA-TGCs may digest ECM proteins and accelerate the invasion of SpA-TGCs into the decidua and their arrival at maternal arteries. Degradation of elastic fibers in arterial walls is another essential step in artery remodeling (Harris and Aplin, 2007; Harris et al., 2010). Mice overexpressing HtrA1 in the retina show damage in the basement membrane of the pigment epithelium and elastic fibers of choroid blood vessels (Jones et al., 2011; Vierkotten et al., 2011), attributed to an elastase activity or a proteolytic activity toward fibulin 5, an essential factor of elestogenesis, of HtrA1. Some HtrA3-expressing cells in the decidua are densely associated with maternal arteries (Fig. S4), and they may contribute to remodeling of the spiral arteries.

Collectively, the defective development of the labyrinth and the junctional zone, impaired arterial remodeling, and intrauterine growth retardation found in *HtrA*$^{-/-}$ mice may be a consequence of abnormal differentiation of SpTs, GlyTCs and SpA-TGCs from *Tpbpa*-positive precursors.

*Tpbpa*-positive lineage cells appear to be preferentially affected in the *HtrA1*$^{-/-}$ placenta. *Pl1*-positive primary P-TGCs, which originate not only from *Tpbpa*-positive precursors but also from *Tpbpa*-negative cells, are not affected (Fig. 7); *Pl2*-positive cells, which also differentiate from both *Tpbpa*-positive and *Tpbpa*-negative cells (Simmons et al., 2007), are increased at E9.5 and E12.5 in the *HtrA1*$^{-/-}$ placenta (Fig. 7). Compensatory mechanisms presumably stimulate differentiation of *Pl2*-positive cells from *Tpbpa*-negative precursors.

The molecular mechanisms underlying the differentiation of various trophoblasts from trophoblast stem (TS) cells are not well characterized. Differentiation of mouse TS cells is known to be regulated by FGF 4 and TGF-$\beta$ (Tanaka et al., 1998; Erlebacher et al., 2004). HtrA1 is an inhibitor of TGF-$\beta$ signaling (Oka et al., 2004; Hara et al., 2009); its expression is induced by FGF during *Xenopus* and chicken development (Hou et al., 2007; Ferrer-Vaquer et al., 2008), and HtrA1 positively regulates FGF signaling in *Xenopus* (Hou et al., 2007). Loss of HtrA1 in TS cells might affect cell fate determination through modification of TGF-$\beta$ and/or FGF signaling. At E7.5, HtrA1 expression began in the EPC, which consists of progenitors of both secondary TGCs and SpTs. Loss of this early expression of HtrA1 in the EPC might affect the cell lineage determination and result in a decrease of *Tpbpa*-positive SpTs and an increase of *Pl2*-positive TGCs. Several soluble factors such as retinoic acid (Yan et al., 2001) and parathyroid hormone related protein (PTHrP) (El-Hashash et al., 2005) are known to stimulate the differentiation of EPC progenitors into TGCs at the expense of SpTs. PTHrP expression is also reportedly induced by TGF-$\beta$ in primary TGCs (Nowak et al., 1999). HtrA1 may therefore suppress PTHrP by inhibiting TGF-$\beta$ signaling. The role of HtrA1 during cell lineage commitment was reported in human bone marrow-derived mesenchymal stem cells, in which HtrA1 enhances osteogenesis but suppresses adipogenesis (Tiaden et al., 2012).

This study provides evidence that HtrA1 regulates trophoblast differentiation and maternal artery remodeling. Lack of artery remodeling due to poor invasion of trophoblasts into the decidua is one of the major pathophysiological mechanisms underlying the onset of PE. The placenta of *HtrA1*$^{-/-}$ mouse shows histological abnormalities very similar to those in BPH/5 preeclampsia model mice (Dokras et al., 2006). MMP-9 null mice show abnormalities in trophoblast differentiation and invasion, and mimic phenotypes of PE (Plaks et al., 2013). Fragments of HtrA1-digested fibronectin induce MMP-1 and MMP-3 production in human synovial fibroblasts (Grau et al., 2006). In murine RPE cells, fibronectin fragments produced by α-chymotrypsin digestion also enhance MMP-9 secretion (Austin et al., 2009). We showed that the *HtrA1*$^{-/-}$ placenta has low MMP-9 activity (Fig. S5), which may be another factor that leads to its histological abnormalities.

More importantly, our data shed light into the debate on the role of HtrA1 in PE. Although there are several reports showing abnormal elevation of HtrA1 in PE, there is no clear evidence yet whether this is a cause of PE or an outcome of a stress response imposed by PE. In addition, HtrA1 expression is frequently decreased in the sera and placentas of PE patients. Our study supports the idea that HtrA1 has important roles in placental development in the early stage of pregnancy, and insufficient HtrA1 expression may cause poor placentation that is depicted by histological abnormalities very similar to those found in the placenta of the PE mouse model. Abnormal phenotypes of the *HtrA1*$^{-/-}$ placenta are mostly accounted for by the embryonic loss of HtrA1 (Fig. S6). HtrA3 in the decidua may compensate for functions of maternal HtrA1. Preliminary data indicate that the double knockout (*HtrA1*$^{-/-}$; *HtrA3*$^{-/-}$) placenta shows similar but more severe phenotypes than the *HtrA1*$^{-/-}$ placenta; in addition, pregnant *HtrA1*$^{-/-}$; *HtrA3*$^{-/-}$ mice display mild hypertension at the later gestation stage, an effect which was not clearly observed in pregnant *HtrA1*$^{-/-}$ mice (M.Z.H., unpublished data).

HtrA proteases in general are stress-responsive factors (Skorko-Glonek et al., 1999; Alba and Gross., 2004; Clausen et al., 2011). HtrA1 is induced by several types of stress such as oxidative stress, UV irradiation, and endoplasmic reticulum stress (Zurawa-Janicka et al., 2008; Ng et al., 2011; Supanji et al., 2013). We have shown that, in mouse embryonic fibroblasts and retinal pigment epithelial cells, oxidative stress-induced HtrA1 confers resistance to cell death but enhances cell senescence (Supanji et al., 2013). HtrA3 is known to be induced by hypoxia in human trophoblast cells (Li et al., 2011), and our preliminary data

indicate that HtrA1 is also induced by hypoxia in mouse embryonic fibroblasts. In early stages of pregnancy, HtrA1 and HtrA3 may be required for the survival and proper differentiation of placental cells under hypoxic conditions. In PE, HtrA1 and HtrA3 expression may remain high through mid-gestation, because of persistent hypoxia. Alternatively, oxidative stress caused by hypoxia-reperfusion insult may induce expression of the HtrA proteases in PE patients. Further analysis is needed to elucidate the precise behavior of HtrA proteases in PE.

## Acknowledgments

We thank Dr. James Cross and Dr. David Simmons for providing plasmid DNAs for RNA probes. Md. Zobaer Hasan was supported by a scholarship from Ministry of Education, Culture, Sports, Science and Technology of Japan.

## Appendix A. Supporting information

Supplementary data associated with this article can be found in the online version at http://dx.doi.org/10.1016/j.ydbio.2014.10.015.

## References

Adamson, S.L., Lu, Y., Whiteley, K.J., Holmyard, D., Hemberger, M., Pfarrer, C., Cross, J.C., 2002. Interactions between trophoblast cells and the maternal and fetal circulation in the mouse placenta. Dev. Biol. 250, 358–373.

Alba, B.M., Gross, C.A., 2004. Regulation of the *Escherichia Coli* sigma-dependent envelope stress response. Mol. Microbiol. 52, 613–619.

Arima, T., Hata, K., Tanaka, S., Kusumi, M., Li, E., Kato, K., Shiota, K., Sasaki, H., Wake, N., 2006. Loss of the maternal imprint in Dnmt3Lmat$^{-/-}$ mice leads to a differentiation defect in the extraembryonic tissue. Dev. Biol. 297, 361–373.

Austin, B.A., Liu, B., Li, Z., Nussenblatt, R.B., 2009. Biologically active fibronectin fragments stimulate release of MCP-1 and catabolic cytokines from murine retinal pigment epithelium. Invest. Ophthalmol. Vis. Sci. 50, 2896–2902.

Baldi, A., De Luca, A., Morini, M., Battista, T., Felsani, A., Baldi, F., Catricala, C., Amantea, A., Noonan, D.M., Albini, A., Natali, P.G., Lombardi, D., Paggi, M.G., 2002. The HtrA1 serine protease is down-regulated during human melanoma progression and represses growth of metastatic melanoma cells. Oncogene 21, 6684–6688.

Carney, E.W., Prideaux, V., Lye, S.J., Rossant, J., 1993. Progressive expression of trophoblast-specific genes during formation of mouse trophoblast giant cells in vitro. Mol. Reprod. Dev. 34, 357–368.

Chen, Y.Y., Chuang, P.Y., Chen, C.P., Chiu, Y.H., Lo, H.F., Cheong, M.L., Huang, J.Y., Kuo, P.L., Chen, H., 2014. Functional antagonism between high temperature requirement protein A (HtrA) family members regulates trophoblast invasion. J. Biol. Chem. 289, 22958–22968.

Chien, J., Staub, J., Hu, S.I., Erickson-Johnson, M.R., Couch, F.J., Smith, D.I., Crowl, R. M., Kaufmann, S.H., Shridhar, V., 2004. A candidate tumor suppressor HtrA1 is downregulated in ovarian cancer. Oncogene 23, 1636–1644.

Clausen, T., Kaiser, M., Huber, R., Ehrmann, M., 2011. HTRA proteases: regulated proteolysis in protein quality control. Nat. Rev. Mol. Cell Biol. 12, 152–162.

Clausen, T., Southan, C., Ehrmann, M., 2002. The HtrA family of proteases: implications for protein composition and cell fate. Mol. Cell 10, 443–455.

Dewan, A., Liu, M., Hartman, S., Zhang, S.S., Liu, D.T., Zhao, C., Tam, P.O., Chan, W.M., Lam, D.S., Snyder, M., Barnstable, C., Pang, C.P., Hoh, J., 2006. HTRA1 promoter polymorphism in wet age-related macular degeneration. Science 314, 989–992.

Dokras, A., Hoffmann, D.S., Eastvold, J.S., Kienzle, M.F., Gruman, L.M., Kirby, P.A., Weiss, R.M., Davisson, R.L., 2006. Severe feto-placental abnormalities precede the onset of hypertension and proteinuria in a mouse model of preeclampsia. Biol. Reprod. 75, 899–907.

Duley, L., 2009. The global impact of pre-eclampsia and eclampsia. Semin. Perinatol. 33, 130–137.

El-Hashash, A.H., Esbrit, P., Kimber, S.J., 2005. PTHrP promotes murine secondary trophoblast giant cell differentiation through induction of endocycle, upregulation of giant-cell-promoting transcription factors and suppression of other trophoblast cell types. Differentiation 73, 154–174.

Erlebacher, A., Price, K.A., Glimcher, L.H., 2004. Maintenance of mouse trophoblast stem cell proliferation by TGF-beta/activin. Dev. Biol. 275, 158–169.

Ferrer-Vaquer, A., Maurey, P., Werzowa, J., Firnberg, N., Leibbrandt, A., Neubuser, A., 2008. Expression and regulation of HTRA1 during chick and early mouse development. Dev. Dyn. 237, 1893–1900.

Fontana, V., Coll, T.A., Sobarzo, C.M., Tito, L.P., Calvo, J.C., Cebral, E., 2012. Matrix metalloproteinase expression and activity in trophoblast-decidual tissues at organogenesis in CF-1 mouse. J. Mol. Histol. 43, 487–496.

Graham, J.R., Chamberland, A., Lin, Q., Li, X.J., Dai, D., Zeng, W., Ryan, M.S., Rivera-Bermudez, M.A., Flannery, C.R., Yang, Z., 2013. Serine protease HTRA1 antagonizes transforming growth factor-beta signaling by cleaving its receptors and loss of HTRA1 in vivo enhances bone formation. PLoS One 8, e74094.

Grau, S., Richards, P.J., Kerr, B., Hughes, C., Caterson, B., Williams, A.S., Junker, U., Jones, S.A., Clausen, T., Ehrmann, M., 2006. The role of human HtrA1 in arthritic disease. J. Biol. Chem. 281, 6124–6129.

Guillemot, F., Caspary, T., Tilghman, S.M., Copeland, N.G., Gilbert, D.J., Jenkins, N.A., Anderson, D.J., Joyner, A.L., Rossant, J., Nagy, A., 1995. Genomic imprinting of Mash2, a mouse gene required for trophoblast development. Nat. Genet. 9, 235–242.

Guillemot, F., Nagy, A., Auerbach, A., Rossant, J., Joyner, A.L., 1994. Essential role of Mash-2 in extraembryonic development. Nature 371, 333–336.

Guillemot, F., Joyner, A.L., 1993. Dynamic expression of the murine achaete-scute homologue Mash-1 in the developing nervous system. Mech. Dev. 42, 171–185.

Hara, K., Shiga, A., Fukutake, T., Nozaki, H., Miyashita, A., Yokoseki, A., Kawata, H., Koyama, A., Arima, K., Takahashi, T., Ikeda, M., Shiota, H., Tamura, M., Shimoe, Y., Hirayama, M., Arisato, T., Yanagawa, S., Tanaka, A., Nakano, I., Ikeda, S., Yoshida, Y., Yamamoto, T., Ikeuchi, T., Kuwano, R., Nishizawa, M., Tsuji, S., Onodera, O., 2009. Association of HTRA1 mutations and familial ischemic cerebral small-vessel disease. N. Engl. J. Med. 360, 1729–1739.

Harris, L.K., Smith, S.D., Keogh, R.J., Jones, R.L., Baker, P.N., Knofler, M., Cartwright, J. E., Whitley, G.S., Aplin, J.D., 2010. Trophoblast- and vascular smooth muscle cell-derived MMP-12 mediates elastolysis during uterine spiral artery remodeling. Am. J. Pathol. 177, 2103–2115.

Harris, L.K., Aplin, J.D., 2007. Vascular remodeling and extracellular matrix breakdown in the uterine spiral arteries during pregnancy. Reprod. Sci. 14, 28–34.

Hou, S., Maccarana, M., Min, T.H., Strate, I., Pera, E.M., 2007. The secreted serine protease xHtrA1 stimulates long-range FGF signaling in the early xenopus embryo. Dev. Cell 13, 226–241.

Hu, D., Cross, J.C., 2011. Ablation of tpbpa-positive trophoblast precursors leads to defects in maternal spiral artery remodeling in the mouse placenta. Dev. Biol. 358, 231–239.

Hu, D., Cross, J.C., 2010. Development and function of trophoblast giant cells in the rodent placenta. Int. J. Dev. Biol. 54, 341–354.

Hu, S.I., Carozza, M., Klein, M., Nantermet, P., Luk, D., Crowl, R.M., 1998. Human HtrA, an evolutionarily conserved serine protease identified as a differentially expressed gene product in osteoarthritic cartilage. J. Biol. Chem. 273, 34406–34412.

Inagaki, A., Nishizawa, H., Ota, S., Suzuki, M., Inuzuka, H., Miyamura, H., Sekiya, T., Kurahashi, H., Udagawa, Y., 2012. Upregulation of HtrA4 in the placentas of patients with severe pre-eclampsia. Placenta 33, 919–926.

Jones, A., Kumar, S., Zhang, N., Tong, Z., Yang, J.H., Watt, C., Anderson, J., Amrita, Fillerup, H., McCloskey, M., Luo, L., Yang, Z., Ambati, B., Marc, R., Oka, C., Zhang, K., Fu, Y., 2011. Increased expression of multifunctional serine protease, HTRA1, in retinal pigment epithelium induces polypoidal choroidal vasculopathy in mice. Proc. Natl. Acad. Sci. USA 108, 14578–14583.

Khan, K.S., Wojdyla, D., Say, L., Gulmezoglu, A.M., Van Look, P.F., 2006. WHO analysis of causes of maternal death: a systematic review. Lancet 367, 1066–1074.

Launay, S., Maubert, E., Lebeurrier, N., Tennstaedt, A., Campioni, M., Docagne, F., Gabriel, C., Dauphinot, L., Potier, M.C., Ehrmann, M., Baldi, A., Vivien, D., 2008. HtrA1-dependent proteolysis of TGF-Beta controls both neuronal maturation and developmental survival. Cell Death Differ. 15, 1408–1416.

Li, Y., Puryer, M., Lin, E., Hale, K., Salamonsen, L.A., Manuelpillai, U., Tong, S., Chan, W., Wallace, E.M., Nie, G., 2011. Placental HtrA3 is regulated by oxygen tension and serum levels are altered during early pregnancy in women destined to develop preeclampsia. J. Clin. Endocrinol. Metab. 96, 403–411.

Lorenzi, T., Marzioni, D., Giannubilo, S., Quaranta, A., Crescimanno, C., De Luca, A., Baldi, A., Todros, T., Tranquilli, A.L., Castellucci, M., 2009. Expression patterns of two serine protease HtrA1 forms in human placentas complicated by pre-eclampsia with and without intrauterine growth restriction. Placenta 30, 35–40.

Marzioni, D., Lorenzi, T., Altobelli, E., Giannubilo, S.R., Paolinelli, F., Tersigni, C., Crescimanno, C., Monsurro, V., Tranquilli, A.L., Di Simone, N., Castellucci, M., 2012. Alterations of maternal plasma HTRA1 level in preeclampsia complicated by IUGR. Placenta 33, 1036–1038.

Marzioni, D., Quaranta, A., Lorenzi, T., Morroni, M., Crescimanno, C., De Nictolis, M., Toti, P., Muzzonigro, G., Baldi, A., De Luca, A., Castellucci, M., 2009. Expression pattern alterations of the serine protease HtrA1 in normal human placental tissues and in gestational trophoblastic diseases. Histol. Histopathol. 24, 1213–1222.

McCarthy, F.P., Kingdom, J.C., Kenny, L.C., Walsh, S.K., 2011. Animal models of preeclampsia; uses and limitations. Placenta 32, 413–419.

Meiner, V.L., Cases, S., Myers, H.M., Sande, E.R., Bellosta, S., Schambelan, M., Pitas, R. E., McGuire, J., Herz, J., Farese Jr, R.V., 1996. Disruption of the Acyl-CoA: cholesterol acyltransferase gene in mice: evidence suggesting multiple cholesterol esterification enzymes in mammals. Proc. Natl. Acad. Sci. USA 93, 14041–14046.

Mould, A., Morgan, M.A., Li, L., Bikoff, E.K., Robertson, E.J., 2012. Blimp1/Prdm1 governs terminal differentiation of endovascular trophoblast giant cells and defines multipotent progenitors in the developing placenta. Genes Dev. 26, 2063–2074.

Mullany, S.A., Moslemi-Kebria, M., Rattan, R., Khurana, A., Clayton, A., Ota, T., Mariani, A., Podratz, K.C., Chien, J., Shridhar, V., 2011. Expression and functional significance of HtrA1 loss in endometrial cancer. Clin. Cancer Res. 17, 427–436.

Nakayama, H., Liu, Y., Stifani, S., Cross, J.C., 1997. Developmental restriction of Mash-2 expression in trophoblast correlates with potential activation of the Notch-2 pathway. Dev. Genet. 21, 21–30.
Ng, T.K., Yam, G.H., Chen, W.Q., Lee, V.Y., Chen, H., Chen, L.J., Choy, K.W., Yang, Z., Pang, C.P., 2011. Interactive expressions of HtrA1 and VEGF in human vitreous humors and fetal RPE cells. Invest. Ophthalmol. Vis. Sci. 52, 3706–3712.
Nie, G., Hale, K., Li, Y., Manuelpillai, U., Wallace, E.M., Salamonsen, L.A., 2006a. Distinct expression and localization of serine protease HtrA1 in human endometrium and first-trimester placenta. Dev. Dyn. 235, 3448–3455.
Nie, G., Li, Y., He, H., Findlay, J.K., Salamonsen, L.A., 2006b. HtrA3, a serine protease possessing an igf-binding domain, is selectively expressed at the maternal-fetal interface during placentation in the mouse. Placenta 27, 491–501.
Nie, G., Li, Y., Salamonsen, L.A., 2005. Serine protease HtrA1 is developmentally regulated in trophoblast and uterine decidual cells during placental formation in the mouse. Dev. Dyn. 233, 1102–1109.
Nie, G.Y., Hampton, A., Li, Y., Findlay, J.K., Salamonsen, L.A., 2003. Identification and cloning of two isoforms of human high-temperature requirement factor A3 (HtrA3), characterization of its genomic structure and comparison of its tissue distribution with HtrA1 and HtrA2. Biochem. J. 371, 39–48.
Nowak, R.A., Haimovici, F., Biggers, J.D., Erbach, G.T., 1999. Transforming growth factor-beta stimulates mouse blastocyst outgrowth through a mechanism involving parathyroid hormone-related protein. Biol. Reprod. 60, 85–93.
Oka, C., Tsujimoto, R., Kajikawa, M., Koshiba-Takeuchi, K., Ina, J., Yano, M., Tsuchiya, A., Ueta, Y., Soma, A., Kanda, H., Matsumoto, M., Kawaichi, M., 2004. HtrA1 serine protease inhibits signaling mediated by Tgfbeta family proteins. Development 131, 1041–1053.
Palei, A.C., Granger, J.P., Tanus-Santos, J.E., 2013. Matrix metalloproteinases as drug targets in preeclampsia. Curr. Drug Targets 14, 325–334.
Plaks, V., Rinkenberger, J., Dai, J., Flannery, M., Sund, M., Kanasaki, K., Ni, W., Kalluri, R., Werb, Z., 2013. Matrix metalloproteinase-9 deficiency phenocopies features of preeclampsia and intrauterine growth restriction. Proc. Natl. Acad. Sci. USA 110, 11109–11114.
Redman, C.W., Sargent, I.L., 2005. Latest advances in understanding preeclampsia. Science 308, 1592–1594.
Rodriguez, T.A., Sparrow, D.B., Scott, A.N., Withington, S.L., Preis, J.I., Michalicek, J., Clements, M., Tsang, T.E., Shioda, T., Beddington, R.S., Dunwoodie, S.L., 2004. Cited1 is required in trophoblasts for placental development and for embryo growth and survival. Mol. Cell Biol. 24, 228–244.
Rossant, J., Cross, J.C., 2001. Placental development: lessons from mouse mutants. Nat. Rev. Genet. 2, 538–548.
Salbaum, J.M., Kruger, C., Zhang, X., Delahaye, N.A., Pavlinkova, G., Burk, D.H., Kappen, C., 2011. Altered gene expression and spongiotrophoblast differentiation in placenta from a mouse model of diabetes in pregnancy. Diabetologia 54, 1909–1920.
Shiga, A., Nozaki, H., Yokoseki, A., Nihonmatsu, M., Kawata, H., Kato, T., Koyama, A., Arima, K., Ikeda, M., Katada, S., Toyoshima, Y., Takahashi, H., Tanaka, A., Nakano, I., Ikeuchi, T., Nishizawa, M., Onodera, O., 2011. Cerebral small-vessel disease protein HTRA1 controls the amount of TGF-beta1 via cleavage of proTGF-beta1. Hum. Mol. Genet. 20, 1800–1810.
Simmons, D.G., Rawn, S., Davies, A., Hughes, M., Cross, J.C., 2008. Spatial and temporal expression of the 23 murine prolactin/placental lactogen-related genes is not associated with their position in the locus. BMC Genom. 9, 352–2164-9-352.
Simmons, D.G., Fortier, A.L., Cross, J.C., 2007. Diverse subtypes and developmental origins of trophoblast giant cells in the mouse placenta. Dev. Biol. 304, 567–578.
Simmons, D.G., Cross, J.C., 2005. Determinants of trophoblast lineage and cell subtype specification in the mouse placenta. Dev. Biol. 284, 12–24.
Skorko-Glonek, J., Zurawa, D., Kuczwara, E., Wozniak, M., Wypych, Z., Lipinska, B., 1999. The *Escherichia Coli* heat shock protease HtrA participates in defense against oxidative stress. Mol. Gen. Genet. 262, 342–350.
Steegers, E.A., von Dadelszen, P., Duvekot, J.J., Pijnenborg, R., 2010. Pre-Eclampsia. Lancet 376, 631–644.
Strauss, K.M., Martins, L.M., Plun-Favreau, H., Marx, F.P., Kautzmann, S., Berg, D., Gasser, T., Wszolek, Z., Muller, T., Bornemann, A., Wolburg, H., Downward, J., Riess, O., Schulz, J.B., Kruger, R., 2005. Loss of function mutations in the gene encoding Omi/HtrA2 in Parkinson's disease. Hum. Mol. Genet. 14, 2099–2111.
Supanji, Shimomachi, M., Hasan, M.Z., Kawaichi, M., Oka, C., 2013. HtrA1 is induced by oxidative stress and enhances cell senescence through p38 MAPK pathway. Exp. Eye Res. 112, 79–92.
Tanaka, M., Gertsenstein, M., Rossant, J., Nagy, A., 1997. Mash2 acts cell autonomously in mouse spongiotrophoblast development. Dev. Biol. 190, 55–65.
Tanaka, S., Kunath, T., Hadjantonakis, A.K., Nagy, A., Rossant, J., 1998. Promotion of trophoblast stem cell proliferation by FGF4. Science 282, 2072–2075.
Tiaden, A.N., Breiden, M., Mirsaidi, A., Weber, F.A., Bahrenberg, G., Glanz, S., Cinelli, P., Ehrmann, M., Richards, P.J., 2012. Human serine protease HTRA1 positively regulates osteogenesis of human bone marrow-derived mesenchymal stem cells and mineralization of differentiating bone-forming cells through the modulation of extracellular matrix protein. Stem Cells 30, 2271–2282.
Tocharus, J., Tsuchiya, A., Kajikawa, M., Ueta, Y., Oka, C., Kawaichi, M., 2004. Developmentally regulated expression of mouse HtrA3 and its role as an inhibitor of TGF-beta signaling. Dev. Growth Differ. 46, 257–274.
Tsuchiya, A., Yano, M., Tocharus, J., Kojima, H., Fukumoto, M., Kawaichi, M., Oka, C., 2005. Expression of mouse HtrA1 serine protease in normal bone and cartilage and its upregulation in joint cartilage damaged by experimental arthritis. Bone 37, 323–336.
Vierkotten, S., Muether, P.S., Fauser, S., 2011. Overexpression of HTRA1 leads to ultrastructural changes in the elastic layer of bruch's membrane via cleavage of extracellular matrix components. PLoS One 6, e22959.
Yan, J., Tanaka, S., Oda, M., Makino, T., Ohgane, J., Shiota, K., 2001. Retinoic acid promotes differentiation of trophoblast stem cells to a giant cell fate. Dev. Biol. 235, 422–432.
Yang, Z., Camp, N.J., Sun, H., Tong, Z., Gibbs, D., Cameron, D.J., Chen, H., Zhao, Y., Pearson, E., Li, X., Chien, J., Dewan, A., Harmon, J., Bernstein, P.S., Shridhar, V., Zabriskie, N.A., Hoh, J., Howes, K., Zhang, K., 2006. A variant of the HTRA1 gene increases susceptibility to age-related macular degeneration. Science 314, 992–993.
Zhao, H., Wong, R.J., Kalish, F.S., Nayak, N.R., Stevenson, D.K., 2009. Effect of heme oxygenase-1 deficiency on placental development. Placenta 30, 861–868.
Zong, L., Wang, L., Huang, P., Shao, W., Song, Y., Gou, W., 2013. High temperature requirement A1 in placental tissues and serum from pre-eclamptic pregnancies with or without fetal growth restriction. Arch. Med. Sci. 9, 690–696.
Zurawa-Janicka, D., Kobiela, J., Stefaniak, T., Wozniak, A., Narkiewicz, J., Wozniak, M., Limon, J., Lipinska, B., 2008. Changes in expression of serine proteases HtrA1 and HtrA2 during estrogen-induced oxidative stress and nephrocarcinogenesis in male syrian hamster. Acta Biochim. Pol. 55, 9–19.